ISSN 2075-1133, Inorganic Materials: Applied Research, 2020, Vol. 11, No. 4, pp. 809–814. © Pleiades Publishing, Ltd., 2020.
Russian Text © The Author(s), 2019, published in Materialovedenie, 2019, No. 10, pp. 19–24.

Magnetic Properties of Bismuth Pyrostannate Doped with 3D Ions

L. V. Udod[a, b, *], S. S. Aplesnin[a, b], and M. N. Sitnikov[b]

[a] *Kirensky Institute of Physics, Krasnoyarsk Scientific Center, Siberian Branch, Russian Academy of Sciences, Krasnoyarsk, 660036 Russia*

[b] *Reshetnev Siberian State University of Science and Technology, Krasnoyarsk, 660037 Russia*

**e-mail: luba@iph.krasn.ru*

Received December 24, 2018; revised March 13, 2019; accepted June 11, 2019

Abstract—The effect of substitution of Cr^{3+} and Mn^{4+} ions for tin in bismuth pyrostannate on the magnetic properties of the compound has been investigated. The interrelation between the magnetic, dielectric, and electrical properties has been established. Qualitative dependences of the temperature behavior of the permittivity and magnetic susceptibility on the substituent ion have been obtained. A change in the conductivity type from hopping to tunneling has been found.

Keywords: crystal structure, magnetic and dielectric properties, *I–V* characteristic, conductivity, phase transitions

DOI: 10.1134/S2075113320040383

1. INTRODUCTION

At present, the compounds with a pyrochlore structure are explored owing to their intriguing ferroelectric and dielectric properties, superconductivity, colossal magnetoresistance, photocatalysis, and metal–semiconductor transition. In most pyrochlore compounds with the general chemical formula A2B2O6O', A and B cations form a sublattice of vertex-sharing tetrahedra, which can lead to the intense frustration of the magnetic interactions. Apparently, for this reason, many pyrochlore compounds exhibit a lack of long-range magnetic order and demonstrate the spin-glass state. Substitution of 3*d*-metal magnetic ions is intensively studied with the prospect of using these compounds as multiferroics and spintronic materials. The interaction of the ion subsystem with the electron subsystem characterized by the spin and orbital magnetic moments is reflected in a variety of physical properties.

Bismuth pyrostannate $Bi_2Sn_2O_7$ is a representative of the pyrochlore family. Its crystal structure undergoes a series of polymorphic transformations: at room temperature, it is a distorted pyrochlore structure, which at 390 K passes from the low-symmetry monoclinic α phase (sp. gr. *P*1*c*1) to the orthorhombic β phase (sp. gr. *Aba*2). This transition [1] is accompanied by the generation of a second harmonic [2]. Above 900 K, one more polymorphic transition to the gg phase (sp. gr. $Fd\bar{3}m$) occurs [1–3].

The electronic configuration of bismuth ions $5d^{10}6s^26p^0$ contains an unshared *s* electron pair. The effect of the unshared bismuth pair causes the high mobility of bismuth and oxygen atoms in the Bi_4O' tetrahedron and their strong shift from the centers of the sites characteristic of an ideal pyrochlore structure. Oxygen ions have two types of environment: one of them is located in the nearest surrounding of bismuth ions and the other is surrounded by tin and bismuth ions.

The aim of this study is to investigate the magnetic properties and establish the magnetic order and interrelation of the magnetic, dielectric, and electric characteristics of the $Bi_2(Sn_{1-x}Me_x)_2O_7$ (Me = Mn, Cr, $x = 0.05, 0.1$) compounds.

2. EXPERIMENTAL

The compounds were fabricated by the solid-state reaction method [4]. The synthesized samples correspond to a monoclinic *Pc* cell in the $Bi_2Sn_2O_7$ α phase [3].

The magnetic properties of the synthesized compounds were examined on a high-temperature device using the Faraday method at temperatures of up to 1100 K in magnetic fields of up to 0.86 T and on a Quantum Design PPMS-9 facility at temperatures of up to 300 K in the field range of $-6\ \text{T} < H < 6\ \text{T}$.

The *I–V* characteristics were obtained with a Kemeterley 6517b electrometer in electric fields from −800 to 800 V/cm.

The capacitance and dissipation factor were determined on an AM-3028 component analyzer in the frequency range of 0.1–1000 kHz at temperatures of 300–750 K.

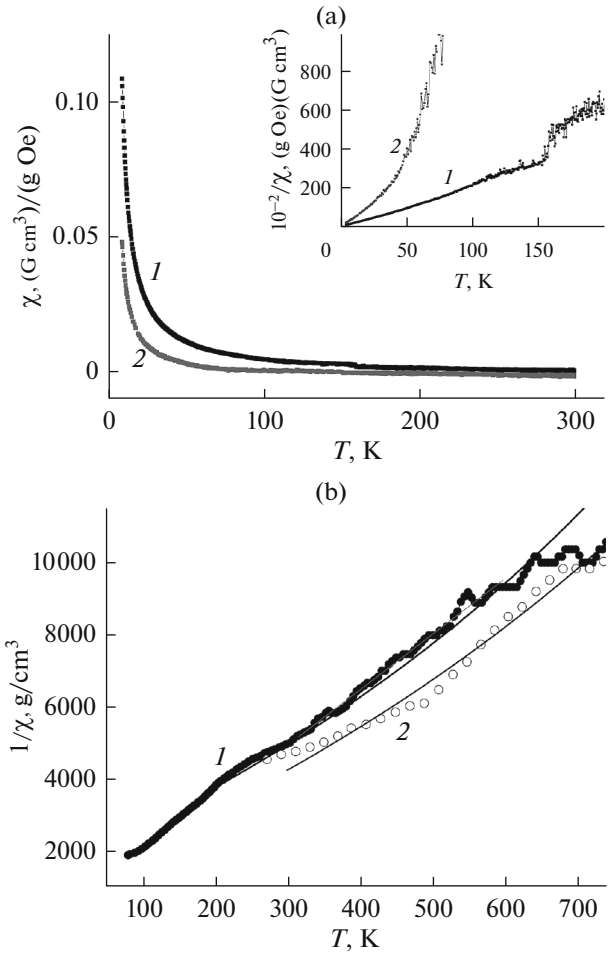

Fig. 1. Temperature dependence of the magnetic susceptibility. (a) $Bi_2(Sn_{0.95}Me_{0.05})_2O_7$ (Me = Mn, Cr): (*1*) $Bi_2(Sn_{0.95}Mn_{0.05})_2O_7$ and (*2*) $Bi_2(Sn_{0.95}Cr_{0.05})_2O_7$. Inset: temperature dependence of the inverse magnetic susceptibility: (*1*) $Bi_{2(}Sn_{0.95}Mn_{0.05})_2O_7$ and (*2*) $Bi_2(Sn_{0.95}Cr_{0.05})_2O_7$. (b) Temperature dependence of the inverse magnetic susceptibility of $Bi_2(Sn_{0.9}Mn_{0.1})_2O_7$: (*1*) experimental results in the sample heating mode; the solid line shows the theoretically calculated $1/\chi_{theor}(T)$ curve; $C = -200$ K; (*2*) experimental results in the sample cooling mode; the solid line shows the theoretically calculated $1/\chi_{theor}(T)$ curve; $C = -150$ K.

3. RESULTS AND DISCUSSION

Magnetic Properties

Figure 1a shows the magnetic susceptibility of the $Bi_2(Sn_{1-x}Me_x)_2O_7$ (Me = Mn, Cr; $x = 0.05$) compound. The magnetic susceptibility of $Bi_2(Sn_{0.95}Cr_{0.05})_2O_7$ at a temperature of 150 K changes its sign from positive to negative. The paramagnetic Curie temperature obtained from the inverse temperature dependence of the magnetic susceptibility (see inset in Fig. 1a) in the range of 0 K < T < 40 K is described by the Curie–Weiss law and has a value of $\theta = 2$ K. The field dependence of the magnetic moment in the field range of -6 T < H < 6 T at $T = 4.2$ K is nonlinear. When it is described by the equation $M(H) = N_A\mu_B SB_S(gS\mu_B H/k_BT)$, where $B_S(x)$ is the Brillouin function, the best agreement with the experimental data is obtained at a chromium ion spin of $S = 3/2$. Here, μ_B is the Bohr magneton, N_A is the Avogadro number, k_B is the Boltzmann constant, and the g factor has a value of $g = 2$. In the $Bi_2(Sn_{0.9}Cr_{0.1})_2O_7$ compound, the magnetic moment increases. The reciprocal magnetic susceptibility curve in the cooling mode changes its slope at the transition from the α to β phase near $T = 370$ K. The paramagnetic Curie temperature increases by a factor of 3; for the α phase, we have $\theta_\alpha = 50$ K in the range of 150 K < T < 300 K, and for the β phase, $\theta_\beta = 150$ K at $T > 400$ K. The temperature dependence of $1/\chi$ is hysteretic in the temperature range of 400–900 K corresponding to the region of existence of the β phase.

The temperature dependence of the $Bi_2(Sn_{0.95}Cr_{0.05})_2O_7$ magnetic susceptibility (Fig. 1a) measured in a magnetic field of 0.05 T has a singularity near 155 K. Using the temperature dependence of the inverse susceptibility (inset in Fig. 1a) described by the Curie–Weiss law, the paramagnetic Curie temperature was found to be $\theta = -0.7$ K. The $M(T)$ curve at a temperature of $T = 4.2$ K is nonlinear, and at $T = 50$ K, the linear dependence described by the Brillouin function is observed.

An increase in the concentration of Mn ions led to an increase in the antiferromagnetic exchange. Figure 1b shows the temperature dependence of the inverse magnetic susceptibility for $Bi_2(Sn_{0.9}Mn_{0.1})_2O_7$ in the sample heating (curve *1*) and cooling (curve *2*) modes. These curves have two points of intersection at temperatures of 270 and 700 K. The nonlinear temperature dependence of the inverse magnetic susceptibility of $Bi_2(Sn_{0.9}Mn_{0.1})_2O_7$ is determined by a sum of two (paramagnetic and diamagnetic) contributions. The inverse magnetic susceptibility $1/\chi_{theor}(T)$ satisfactorily describes the experimental results at $C = 1.36$ K for the heating and cooling modes. The paramagnetic Curie temperature is $\theta = -200$ K in the low-temperature phase and $\theta = -150$ K in the high-temperature phase. The effective magnetic moment with a g factor smaller than 2 calculated using the formula $\mu = \sqrt{8C} = 3.3\mu_B$ is 13% smaller than its theoretical value $\mu_{theor} = 3.8$ found from the relation $\mu_{theor} = qpS(S+1)$ (S is the Mn^{+4} ion spin, $S = 3/2$, and $g = 2$). The distortion of the Bi_4O tetrahedron decreases the g factor.

Permittivity

The spectral and temperature dependences of the permittivity can be used to detect the electric dipole moment and determine its characteristics, even when it concerns the local dipole moment in small clusters without long-range order.

The frequency and temperature dependences of the permittivity of the $Bi_2(Sn_{0.95}Me_{0.05})_2O_7$ (Me = Mn, Cr) compound contain no noticeable anomalies. With an increase in the substituent ion concentration, the anomalies in the form of broad maxima of the dissipation factor arise, the temperature of which increases logarithmically with frequency.

The temperature dependence of the $Bi_2Sn_2O_7$ permittivity exhibits the anomalies described in the model of martensitic phase transitions [5, 6]. The real and imaginary parts of the $Bi_2(Sn_{0.9}Cr_{0.1})_2O_7$ permittivity as a function of temperature at different frequencies are shown in Fig. 2. The $\varepsilon(T)$ dependences contain inflection points in the real part (Fig. 2a) and broad maxima of the dissipation factor (Fig. 2b), the temperature of which increases with frequency from T_M = 370 to 560 K according to the logarithmic law. The dipole moment relaxation time obeys the Arrhenius law $\tau = \tau_0\exp(\Delta E/kT)$ with an activation energy of $\Delta E = 0.4$ eV, which describes the relaxation in disordered systems. When tin is replaced by 3*d* ions, bismuth ions shift from the ring center with the formation of electric dipole moments. In the glass state, the system of dipoles randomly distributed over a rigid isotropic matrix is disordered and unpolarized, but this state is not paraelectric either, since each dipole remembers its initial orientation. Further heating led to a sharp increase in the permittivity upon approaching the temperature of the phase transition $\beta \rightarrow \gamma$.

A criterion of the transition of the system to the dipole glass state is the specific dependence of the dispersion of the real (Re(ε')) and imaginary (Im(ε")) parts of the complex permittivity near the temperature of the transition to the glass phase [7].

At $x = 0.05$, dipole clusters with short-range order and a thermodynamic mean zero dipole moment $p_i = 0$ are formed. The effect of the short-range order manifests itself in the change in the frequency dependence of the complex permittivity, which can be approximated by the power function $\varepsilon = A/\omega^n$ to 10^5 Hz, and at higher frequencies, the permittivity decreases more abruptly. The dispersion of the real part of the permittivity in the monoclinic phase is no more than 10% and the dielectric loss decreases by several times. Upon the transition to the trigonal phase, the dispersion increases and the exponent grows from $n = 0.05$ to 0.4.

In the $Bi_2(Sn_{0.9}Cr_{0.1})_2O_7$ compound, the real and imaginary parts of the permittivity have a broad maximum, which shifts toward higher temperatures with increasing frequency (Fig. 2). The $\varepsilon(\omega)$ dependences are not described in the Debye and Cole–Cole models. If we introduce the frequency dependence of the relaxation time, then, using the Debye expression for $\varepsilon(\omega, T)$, we can describe the experimental results. Along with indefinitely long relaxation times in glasses, the system has a large set of finite relaxation times; i.e., the relaxation time range is wide. In bismuth pyrostannates, there is a relaxation time spectrum caused by the ion- and electron-relaxation polarization. A change in the relaxation mechanism is observed around 100 kHz.

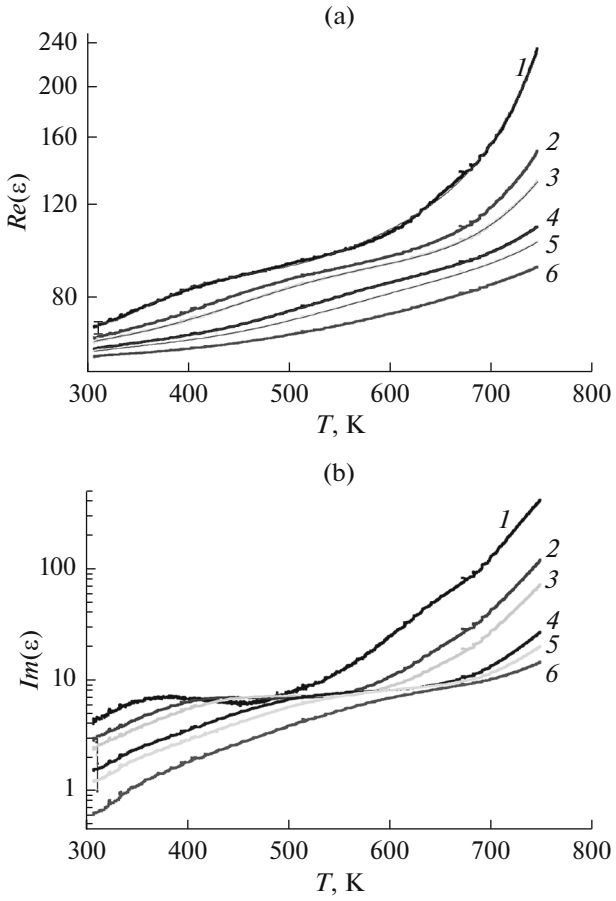

Fig. 2. Temperature dependence of the permittivity of $Bi_2(Sn_{0.9}Cr_{0.1})_2O_7$ at different frequencies. (a) Real and (b) imaginary parts: (*1*) 1, (*2*) 5, (*3*) 10, (*4*) 50, (*5*) 100, and (*6*) 300 kHz.

Above 600 K, the imaginary part of the permittivity is well described by the dependence $\ln(Im(\varepsilon)) = A + \Delta E/T$ with the activation energy which is almost frequency- and concentration-independent and amounts to $\Delta E = 0.82(2)$ eV. The contribution of carriers to the dielectric loss can be ignored, since the relation $\omega Im(\varepsilon) = \sigma$ is invalid. For the composition with $x = 0.05$, this is fundamentally different from the temperature behavior of the dc resistance, which weakly changes at these temperatures. This allows us to conclude that the dielectric loss and the permittivity growth are caused by the ionic subsystem and result from the high mobility of bismuth ions in the pyrostannate structure in the region of the transition $\alpha \rightarrow \beta$.

The real part of the permittivity *Re*(ε) of $Bi_2(Sn_{0.9}Mn_{0.1})_2O_7$ (Fig. 3a) has a small minimum in the vicinity of the phase transition $\alpha \rightarrow \beta$, above which the permittivity sharply increases. These anomalies

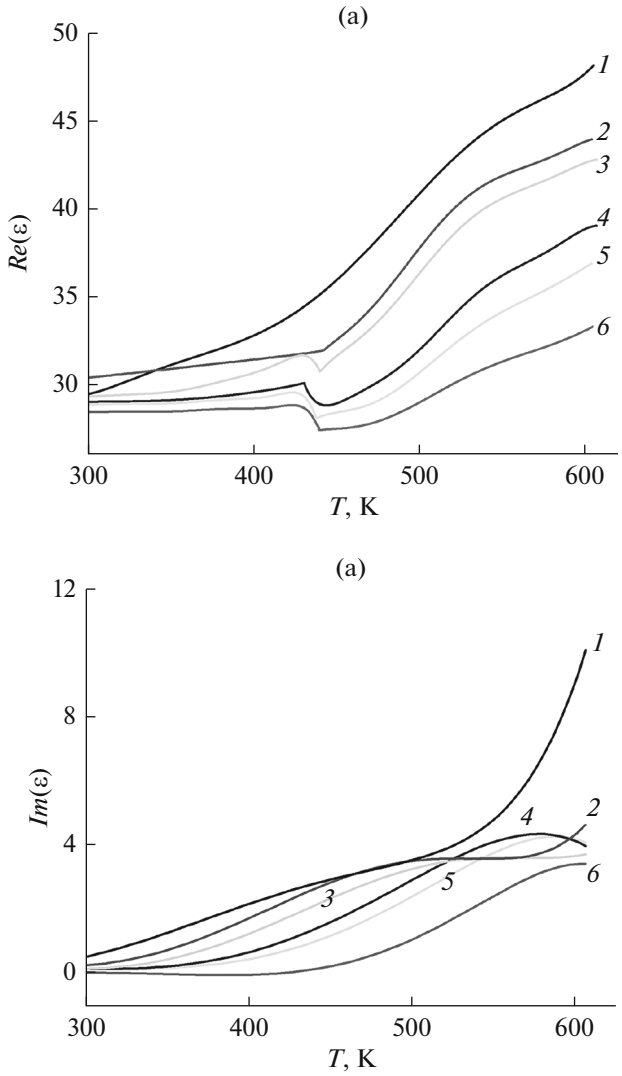

Fig. 3. Temperature dependence of the permittivity of $Bi_2(Sn_{0.9}Mn_{0.1})_2O_7$ at different frequencies. (a) Real and (b) imaginary parts: (*1*) 1, (*2*) 5, (*3*) 10, (*4*) 50, (*5*) 100, and (*6*) 300 kHz.

are consistent with the differential scanning calorimetry data; there is a small singularity on the DSC curve at $T = 420$ K [8]. The real and imaginary parts of the permittivity exhibit a broad maximum at $T > 500$ K (Fig. 3), which are not observed in the DSC curve. A similar temperature dependence of the permittivity above $T = 550$ K is observed in the $Bi_2(Sn_{0.9}Cr_{0.1})_2O_7$ compound.

The high-temperature behavior of the permittivity is related to the electronic structure because of the high electron polarizability of the Bi–O bond. It is well known that oxygen ions have significant polarizability, which increases with the formation of a covalent bond (the presence of covalence and anisotropy). The polarizability of bismuth ions arises from unshared $6s^2$ valence electron pairs. The effect of a single pair enhances the mobility of oxygen ions in the Bi_4O tetrahedron and their great shift from the sites of the ideal pyrochlore lattice. The absence of significant structural changes in $Bi_2Sn_2O_7$ in the temperature range of 500–600 K gives us grounds to assume that the observed features of the dielectric susceptibility are caused by the charge transfer processes and the sharp change in the polarizability of ions [8]. A similar behavior of the permittivity was observed in α-Bi_2O_3 [9]. Substitution of Cr and Mn ions for Sn ions leads to the deformation of the oxygen–bismuth bond and an increase in the dipole moment because of the difference between the ionic radii. The heterovalent substitution of chromium for tin ions causes the electronic contribution to the dielectric susceptibility and an increase in the $Re(\varepsilon)$ value as compared with the substitution of manganese ions with the ionic contribution. According to the experimental data, the $Bi_2(Sn_{0.9}Me_{0.1})_2O_7$ (Me = Mn, Cr) compounds exhibit the properties of a dipole glass.

Conductivity

The conduction mechanism and the existence of inhomogeneous electronic states can be determined from the *I–V* characteristics of the $Bi_2(Sn_{0.9}Me_{0.1})_2O_7$ (Me = Mn, Cr) compositions (Fig. 4). With increasing temperature, the shape of the *I–V* curve changes. In the temperature range of charge ordering, the conductivity is described by the model of space-charge-limited currents and obeys the quadratic Mott law [10]

$$j = \frac{9}{8}\tau_\mu \sigma_0 \mu \frac{U^2}{L^3}, \quad (1)$$

where J is the current density, τ_μ is the Maxwell relaxation time, σ_0 is the electrical conductivity in the bulk of the material in the absence of carrier injection, μ is the carrier mobility, U is the applied voltage, and L is the sample thickness. The experimental *I–V* characteristics in logarithmic coordinates (Fig. 4a) are described well by Eq. (1) for $Bi_2(Sn_{0.9}Mn_{0.1})_2O_7$ up to $T = 400$ K and for $Bi_2(Sn_{0.9}Cr_{0.1})_2O_7$ up to $T = 500$ K. In the high-temperature region, starting with $T = 450$ K for $Bi_2(Sn_{0.9}Mn_{0.1})_2O_7$ and 550 K for $Bi_2(Sn_{0.9}Cr_{0.1})_2O_7$, the Poole–Frenkel conduction mechanism prevails (Fig. 4b), according to which a strong electric field applied to a sample changes the form of potential barriers for carriers between atoms in a crystal lattice. This leads to an increase in the number of electrons in a sample owing to overcoming the potential barrier. In this case, the current exponentially depends on the applied voltage and there is a square root of the voltage in the exponent:

$$I = e\mu n_0 \frac{U}{L} \exp \frac{\beta U^{1/2}}{kTL^{1/2}}, \quad (2)$$

where e is the elementary charge, μ is the carrier mobility, n_0 is the electron density in the conduction

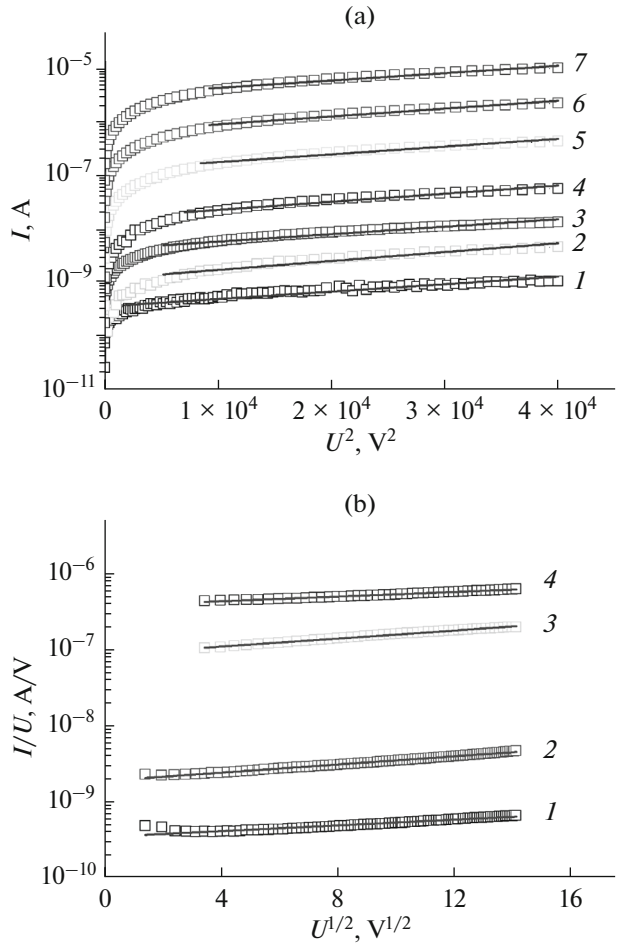

Fig. 4. *I–V* characteristics of $Bi_2(Sn_{0.9}Me_{0.1})_2O_7$ (Me = Mn, Cr) at an applied positive voltage. (a) Dependence of the current on the squared voltage: (*1*) $Bi_2(Sn_{0.9}Mn_{0.1})_2O_7$ at T = 350 K, (*2*) $Bi_2(Sn_{0.9}Cr_{0.1})_2O_7$ at T = 300 K, (*3*) $Bi_2(Sn_{0.9}Mn_{0.1})_2O_7$ at T = 400 K, (*4*) $Bi_2(Sn_{0.9}Cr_{0.1})_2O_7$ at T = 350 K, (*5*) $Bi_2(Sn_{0.}9Cr_{0.1})_2O_7$ at T = 400 K, (*6*) $Bi_2(Sn_{0.9}Cr_{0.1})_2O_7$ at T = 450 K, and (*7*) $Bi_2(Sn_{0.9}Cr_{0.1})_2O_7$ at T = 500 K. (b) *I–V* characteristics in the Poole–Frenkel representation: (*1*) $Bi_2(Sn_{0.9}Mn_{0.1})_2O_7$ at T = 450 K, (*2*) $Bi_2(Sn_{0.9}Mn_{0.1})_2O_7$ at T = 500 K, (*3*) $Bi_2(Sn_{0.9}Cr_{0.1})_2O_7$ at T = 550 K, and (*4*) $Bi_2(Sn_{0.9}Cr_{0.1})_2O_7$ at T = 600 K.

band in zero field, U is the applied voltage, L is the sample thickness, k is the Boltzmann constant, $\beta = \left(\frac{e^3}{\pi\varepsilon\varepsilon_0}\right)^{1/2}$ is the Poole–Frenkel constant, ε_0 is the dielectric constant, and ε is the permittivity of a semiconductor. The linearity of the portions in the dependence of $\ln(I/U)$ on $U^{1/2}$ in the Poole–Frenkel coordinates indicates that the dominant carrier transport occurs via both the hopping mechanism and tunnel electron emission [11]. With an increase in the substituent ion concentration in the $Bi_2(Sn_{0.85}Cr_{0.15})_2O_7$ compound [4], the conduction mechanism does not change, but the transition to the Poole–Frenkel mechanism is observed at a lower (T = 450 K) temperature.

4. CONCLUSIONS

The $Bi_2(Sn_{1-x}Me_x)_2O_7$ (Me = Mn, Cr; x = 0.05) compounds with a monoclinic structure were synthesized by the solid-phase reaction. The experimental investigations showed the interrelation of their structural, magnetic, and electrical properties. The structural transition $\alpha \rightarrow \beta$ is accompanied by anomalies in the temperature behavior of the magnetic susceptibility. In the $Bi_2(Sn_{1-x}Mn_x)_2O_7$ compound, the antiferromagnetic exchange prevails, while in the $Bi_2(Sn_{1-x}Cr_x)_2O_7$, the ferromagnetic exchange is dominant. In the high-temperature phase, the exchange interaction in these compounds increases. The magnetic measurements confirmed that chromium ions are trivalent and manganese ions are tetravalent. The magnetic susceptibility anomalies correlate with the data of the dielectric and electrical measurements. The conduction mechanism was explained using the Poole–Frenkel model and the hopping type of conductivity. The electronic transition with the change in the type of conductivity from the hopping to Poole–Frenkel tunnel emission type is accompanied by the maximum dielectric susceptibility. The temperatures of the transition related to the change in the conduction mechanism from Mott to Poole–Frenkel type are different for the $Bi_2(Sn_{0.9}Cr_{0.1})_2O_7$ and $Bi_2(Sn_{0.9}Mn_{0.1})_2O_7$ compounds. An analysis of the frequency and temperature dependence of the dielectric susceptibility revealed the spin glass state of the $Bi_2(Sn_{0.9}Me_{0.1})_2O_7$ (Me = Mn, Cr) compound. The polarization relaxation is described by a power and logarithmic dependence.

FUNDING

This study was supported by the Russian Foundation for Basic Research, project nos. 18-52-00009 Bel_a, 18-42-240001 r_a, and 18-32-00079 mol_a and state assignment no. 3.5743.2017/6.7.

CONFLICT OF INTEREST

The authors declare that they have no conflict of interest.

REFERENCES

1. Lewis, J.W., Payne, J.L., Evans, I.R., Stokes, H.T., Campbell, B.J., and Evans, J.S.O., An exhaustive symmetry approach to structure determination: phase transitions in $Bi_2Sn_2O_7$, *J. Am. Chem. Soc.*, 2016, vol. 138, pp. 8031–8042. https://doi.org/10.1021/jacs.6b04947
2. Kahlenberg, V. and Zeiske, Th., Structure of γ-$Bi_2Sn_2O_7$ by high temperature powder neutron dif-

fraction, *Z. Kristallogr.*, 1997, vol. 212, pp. 297–301. https://doi.org/10.1524/zkri.1997.212.4.297

3. Evans, I.R., Howard, J.A.K., and Evans, J.S.O., α-$Bi_2Sn_2O_7$—a 176 atom crystal structure from powder diffraction data, *J. Mat. Chem.*, 2003, vol. 13, no. 9, pp. 2098–2103. https://doi.org/10.1039/B305211G
4. Aplesnin, S.S., Udod, L.V., and Sitnikov, M.N., Electronic transition, ferroelectric and thermoelectric properties of bismuth pyrostannate $Bi_2(Sn_{0.85}Cr_{0.15})_2O_7$, *Ceram. Int.*, 2018, vol. 44, pp. 1614–1620. https://doi.org/10.1016/j.ceramint.2015.12.040
5. Udod, L.V., Aplesnin, S.S., Sitnikov, M.N., and Molokeev, M.S., Dielectric and electrical properties of polymorphic bismuth pyrostannate $Bi_2Sn_2O_7$, *Phys. Solid State*, 2014, vol. 56, no. 7, pp. 1315–1319.
6. Maltseva, L.A., Vakhonina, K.D., Levina, A.V., Maltseva, T.V., and Sharapova, V.A., Properties and phase transformations progressing in complex alloyed stainless austenitic steel upon heating, *Inorg. Mater.: Appl. Res.*, 2017, vol. 8, no. 1, pp. 176–180.
7. Rudkovskaya, L.M., Rudkovskii, V.N., Sakhnenko, V.P., and Grunskii, O.S., Flux crystallization of $Pb(Mg_{1/3}Nb_{2/3})O_3$ single crystals by the Czochralski method, *Crystallogr. Rep.*, 2014, vol. 59, no. 2, pp. 284–287. https://doi.org/10.1134/S1063774514020175
8. Aplesnin, S.S., Udod, L.V., Sitnikov, M.N., Molokeev, M.S., Tarasova, L.S., and Yanushkevich, K.I., Magnetic, dielectric, and transport properties of bismuth pyrostannate $Bi_2(Sn_{0.9}Mn_{0.1})_2O_7$, *Phys. Solid State*, 2017, vol. 59, pp. 2268–2273. https://doi.org/10.1134/S1063783417110038
9. Weber, M., Schlesinger, M., Walther, M., Zahn, D., Schalley, C.A., and Mehring, M., Investigations on the growth of bismuth oxido clusters and the nucleation to give metastable bismuth oxide modifications, *Z. Kristallogr.*, 2017, vol. 232, pp. 185–207. https://doi.org/10.1515/zkri-2016-1970
10. Shiryaev, A.A., Vorotyntsev, V.M., and Shobolov, E.L., Poole–Frenkel effect and the opportunity of its application for the prediction of radiation charge accumulation in thermal silicon dioxide, *Semiconductors*, 2018, vol. 52, no. 9, pp. 1114–1117. https://doi.org/10.1134/S1063782618090166
11. Ushakov, A.V., Barshutina, M.N., and Barshutin, S.N., Investigation of the efficiency of resonant tunneling method to control the concentration of fullerenes in organosilicon composites, *Vestn. Tambov. Gos. Tekh. Univ.*, 2015, vol. 21, pp. 526–531. https://doi.org/10.17277/vestnik.2015.03.pp.526-531

Translated by E. Bondareva